Taylor & Francis
Taylor & Francis Group

Electric transport properties of Pt/Permalloy bilayers in the presence of an external magnetic field

Peter Weinberger[ab]*

aCenter for Computational Nanoscience, Seilerstätte 10/22, Vienna, A-1010 Austria; bDepartment of Physics, New York University, 4 Washington Place, New York, NY 10003, USA

A recent experimental study of the electric properties of Pt/Permalloy bilayers based on a simultaneous application of an in-plane microfrequency current and an external magnetic field is simulated on a fully relativistic *ab initio* level by considering the resistivity as an implicit function of the free energy. It is found that the oscillations detected experimentally are caused by the different behavior of out-of-plane and in-plane resistivities in the vicinity of that value of the free energy that corresponds to the resonant field induced by the applied current. A necessary precondition for such oscillations is a sizeable perpendicular anisotropy, which is not the case in systems consisting only of Permalloy. It is shown that the observed phenomenon is essentially an interface effect.

Keywords: anisotropic properties; electrical properties; electrical transport; interfaces; magnetic anisotropy; spin dynamics; magnetic films; magnetic multilayers; spintronics

1. Introduction

Recently a very interesting study of Pt/Permalloy (Permalloy = Py) bilayers sealed with a Ta cap of 1 nm width was presented [1] in which an in-plane microwave frequency current was applied that led to oscillations in the bilayer resistance when an external magnetic field of particular strength was present. The interpretation of the results given was based on a phenomenological Landau–Lifshitz–Gilbert equation augmented by an additional "spin torque" and an additional "Oersted field" term. Since it was said right at the beginning in [1] that the whole effect is due to "spin–orbit scattering", it is quite tempting to simulate this experiment using a fully relativistic *ab initio* approach, i.e., an approach based on the Dirac equation, by evaluating the resistivity in these systems as a function of the applied external magnetic field. It will be shown that (i) the measured spectra (Figure 2a, c and d in [1]) can be explained quantitatively correct considering the interplay between out-of-plane and in-plane resistivities, and (ii) that the discovered phenomenon is essentially caused by an interface effect. In particular it will also be explained why

---

*Email: weinberger@computational-nanoscience.de

experimentally investigated Py films not connected to Pt do not show such oscillations.

2. Investigated systems

Since some of the experimental samples were of the type Pt[x nm]Py[4 nm]Ta[1 nm], in order to simulate the experimental results as close as possible, free-standing films of the type Pt[x nm]Py[3.9 nm]Ta[1 nm], $x = 2.5$, 3.7, Py $= Ni_{80}Fe_{20}$, were considered. It should be noted that such free-standing films can be described selfconsistently correct by stacking together, e.g., semi-infinite systems of the type Py(111)/Vac, Py(111)/Ta and Py(111)/Pt assuming that the interior of the Py layers is bulk-like. Thus, in terms of monolayers with an interlayer spacing as in bulk fcc $Ni_{80}Fe_{20}$(111), selfconsistent scattering potentials for systems such as vac/Pt_n/Py_6[Py-bulk]$_7$$Py_6$$Ta_5$/ vac can be easily obtained. All calculations were performed in terms of the spin-polarized relativistic screened Korringa–Kohn–Rostoker method using the inhomogeneous coherent potential approximation [2,3] and by means of an equivalent fully relativistic Kubo equation [2,3] applying the same numerical set-up as described in [4,5]. It should be noted that of course in a fully relativistic approach, i.e., by using the Dirac equation, "spin-orbit interactions" are described properly to all orders of the inverse speed of light.

3. Theoretical approach

At a given thickness of Py, the Ta cap, and of the Pt layer, the free energy $\Delta E(\Theta, \Phi)$ with respect to a uniform orientation of the magnetization parallel to the surface normal (along the z-axis) is given by

$$\Delta E(\Theta, \Phi) = E(\Theta, \Phi) - E(0, 0), \tag{1}$$

where $E(\Theta, \Phi)$ denotes the grand canonical potential [2] for given values of Θ and Φ with Θ denoting a (clockwise) rotation of the orientation of the magnetization around the (in-plane) y-axis, and Φ referring to such a rotation around the z-axis. As discussed elsewhere, [2,3] these free energies can be viewed layerwise,

$$\Delta E(\Theta, \Phi) = \sum_{i=1,N} \Delta E_i(\Theta, \Phi), \tag{2}$$

with N being the total number of atomic layers in a particular system. The individual $\Delta E_i(\Theta, \Phi)$ pin-point from which part of the system the main contributions to $\Delta E(\Theta, \Phi)$ arise.

Assuming that the experimentally recorded in-plane current flows in the direction of the in-plane x-axis, $j_x(\Theta, \Phi) = \sigma_{xx}(\Theta, \Phi)E_x$, where $\sigma_{xx}(\Theta, \Phi)$ is the xx-element of the conductivity tensor, and $E_x = E$ is the electric field, then in accordance with Equation (2) the following differences in the xx-like elements of resistivity tensors can be defined,

$$\Delta \rho_{xx}(\Theta, \Phi) = \rho_{xx}(\Theta, \Phi) - \rho_{xx}(0, 0), \tag{3}$$

with $\rho_{xx}(\Theta, \Phi) = [\sigma_{xx}(\Theta, \Phi)]^{-1}$. It should be noted that $\Delta E(\Theta, \Phi)$ and $\Delta\rho_{xx}(\Theta, \Phi)$ form surfaces in a space spanned by Θ and Φ.

Since to any given pair of angles Θ and Φ a mapping between $\Delta E(\Theta, \Phi)$ and $\Delta\rho_{xx}(\Theta, \Phi)$ can be established ($f : \Delta E(\Theta, \Phi) \to \Delta\rho_{xx}(\Theta, \Phi)$) the difference resistivity $\Delta\rho_{xx}(\Theta, \Phi)$ versus $\Delta E(\Theta, \Phi)$ can be displayed, i.e., as an implicit function of monotonously increasing values of the free energy. Furthermore, since the free energy is proportional to the magnitude of the applied external magnetic field H, it is in particular useful to view the resistivity difference as a graphical solution of the implicit dependence of the resistivity difference on H, $\Delta\rho_{xx}(H)$.

4. Py-only and Py/Ta systems

As can be seen from Figure 1 in all the three cases displayed there the most stable state corresponds to an in-plane orientation of the magnetization. Already a tiny external magnetic field leads to a perpendicular orientation of the magnetization at which per definition no in-plane rotational degrees of freedom exist, and therefore in Figure 1 $\Delta\rho_{xx}(0, \Phi) = \Delta\rho_{xx}(0, 0)$ $\forall\Phi$. Quite clearly by increasing the external magnetic field beyond the value that corresponds to $\Delta E(0, 0)$, i.e. beyond the energetically highest magnetic configuration, the difference resistivity remains constant. It is perhaps interesting to note that the perpendicular anisotropy of a free-standing Py film of 4 nm width is only by a factor of about 2 larger than the corresponding in-plane anisotropy.

5. Py/Pt systems

The situation is completely different once Py is connected to Pt. In Figure 2 cuts of the $\Delta E(\Theta, \Phi)$ and the $\Delta\rho_{xx}(\Theta, \Phi)$ surfaces with the xz- and the xy-plane, respectively, are displayed. As can be seen from Figure 2a the most stable state refers to a perpendicular orientation of the magnetization. Applying an external field first leads to an orientation of the magnetization along x (xz-plane) entering there the energy regime of in-plane anisotropies (xy-plane). Since z was chosen to be parallel to the surface normal, namely (111), the cut with the xy-plane shown in Figure 2b reflects the in-plane $\mathcal{C}_3$ symmetry of the system. Although at $\Theta = 90$ the variation of the free energy with respect to Φ is rather tiny, namely of the order of μeV, the changes in the resistivities are remarkable: Moving first along the path $[\Theta, 0]$ the resistivity increases (xz-plane) while along $[90, \Phi]$ (xy-plane) it decreases.

As perhaps can be guessed the difference between the $\Delta E(\Theta, 0)$ in Figures 1 and 2 is mainly caused by different interface effects. In Figure 3 the layer-resolved free energies, see Equation (2), are shown for Py[4 nm]Ta[1 nm] with and without a Pt cap of 2.5 nm thickness. It is obvious from this figure that the free energy (the sum over all layer-resolved contributions) is determined almost exclusively by the interfaces between Py and the adjacent media. The Pt/Py interface causes a very strong positive contribution to $\Delta E(90, 0)$ and is therefore responsible for the perpendicular orientation of the magnetization in this system. Figure 3 shows impressively that the sign and the size of the free energy $\Delta E(\Theta, 0)$ in these bilayer systems is essentially governed by the interfaces.
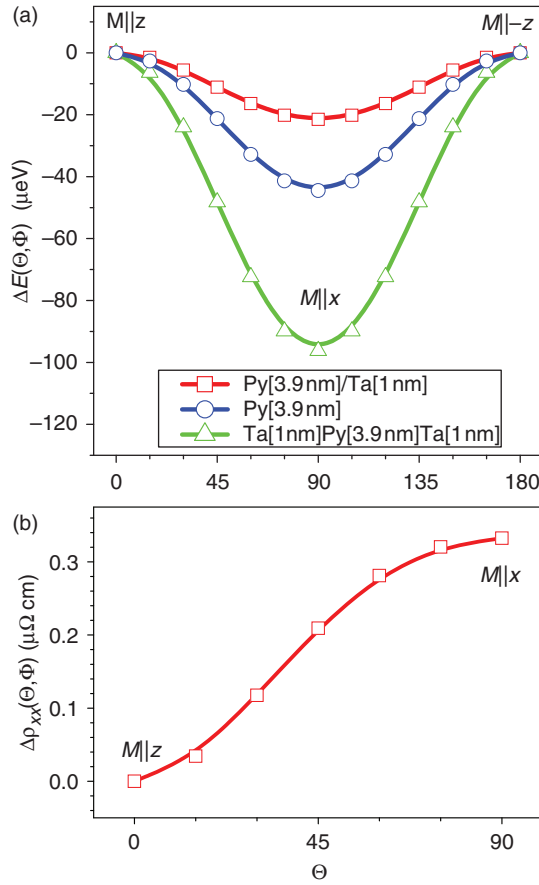
Figure 1. (Color online). (a) $\Delta E(\Theta, 0)$ for Py[3.9 nm]Ta[1 nm] (□), Py[3.9nm] (○) and Ta[1 nm]Py[3.9 nm]Ta[1 nm] (△), see also Equation (1). Note that in all three cases the minimum in the free energy refers to an in-plane orientation of the magnetization (along x). (b) $\Delta \rho_{xx}(\Theta, 0)$ for Py[3.9 nm]Ta[1 nm]. Special orientations of the magnetization (M) are marked explicitly.

5.1. *Temporal aspects*

Since the derivative of the free energy with respect to the direction of the magnetization is nothing but the internal energy in the Landau–Lifshitz–Gilbert equation, the precessional term in this equation can be used [3] to estimate the time ("switching time") needed to move along a particular path on the free energy surface from one magnetic configuration to another one. It turns out that the switching time along a path of constant Φ is by about 3 orders of magnitude faster than along a path of constant Θ. For example, by using a Gilbert damping factor of 1 for the system with a Pt thickness of 2.5 nm, to switch from $\Theta = \Phi = 0$ (perpendicular arrangement) to $\Theta = 90$, $\Phi = 0$ (in-plane) only about 0.03 ns are needed, while from $\Theta = 90$, $\Phi = 0$ to $\Theta = 90$, $\Phi = 30$, see also Figure 2, the switching time amounts
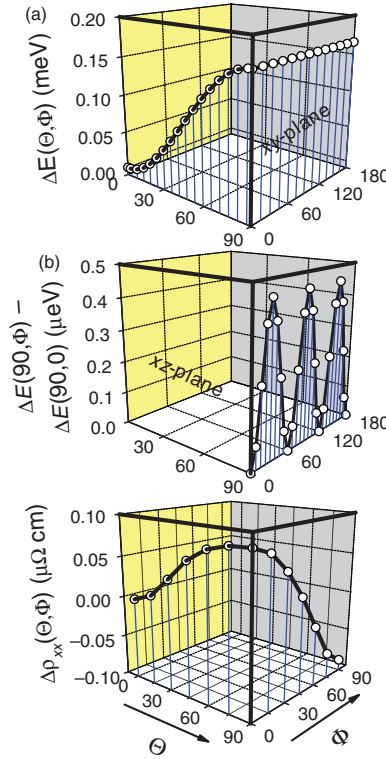
Figure 2. (Color online). Pt[3.7 nm]Py[3.9 nm]Ta[1 nm]. Cuts of the $\Delta E(\Theta, \Phi)$ and $\Delta\rho_{xx}(\Theta, \Phi)$ surfaces with the *xz*- and *xy*-plane. (b) Cut with the *xy*-plane using an appropriate energy scale.

to 36 ns. It should be noted that of course the mentioned difference in time scales does not depend on the actual value for the Gilbert damping factor.

6. Comparison to experiment

Experimentally a resonance line is observed whenever the external magnetic field H approaches the resonant field H_0 corresponding to the applied microwave current, i.e., whenever $H_0 \sim H$, see in particular Equation (2) in [1]. In Figure 4a the angle Θ versus $\Delta E(\Theta, 0)$ is displayed in the case of Pt[3.7 nm]Py[3.9 nm]Ta[1 nm]. In using the calibration of H_0 with respect to the resonance frequency given in [1], one can immediately see that different frequencies refer to different out-of-plane-type orientations of the magnetization (it should be noted that any direction specified by Θ and Φ is "out-of-plane", if $\Theta \neq 90$, and "in-plane", if $\Theta = 90$. In-plane configurations ($\Theta = 90$, $0 \le \Phi \le 180$) correspond to a frequency of about 8.5 GHz.
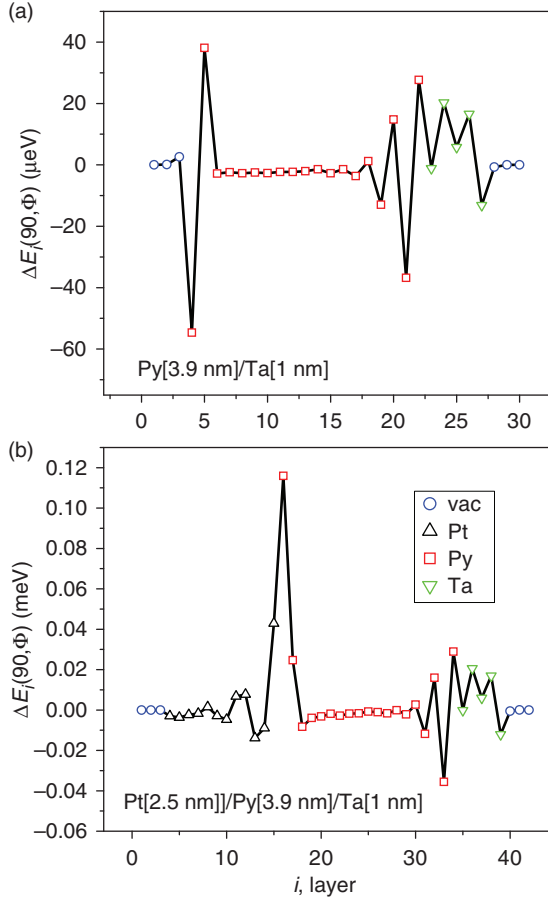
Figure 3. (Color online). Layer-resolved free energies $\Delta E_i(90, 0)$, see Equation (2) for Py[3.9 nm]Ta[1 nm] (a) and Pt[2.5 nm]Py[3.9 nm]Ta[1 nm] (b). The various types of atomic layers are marked explicitly. Note the difference in the scale on the ordinate.

By displaying $\Delta\rho_{xx}(\Theta, 0)$ versus $\Delta E(\Theta, 0)$, $0 \leq \Theta \leq 90$, and $\Delta\rho_{xx}(90, \Phi)$ versus $\Delta E(90, \Phi)$, $0 \leq \Phi \leq 30$, i.e., by considering the difference resistivity along the paths shown in Figure 2 as an implicit function of monotonously increasing free energy H, $\Delta\rho_{xx}(H)$,

$$H = \begin{cases} \Delta E(\Theta, 0), & 0 \leq \Theta < 90; \text{ cut with the } xz\text{-plane}, \\ \Delta E(90, \Phi), & 0 \leq \Phi \leq 30; \text{ cut with the } xy\text{-plane}, \end{cases} \qquad (4)$$

a rather surprising view is obtained, see Figure 4. Increasing H from zero up to the point at which the configuration along the in-plane x-axis is reached ($\Theta = 90$, $\Phi = 0$) the difference resistivity increases (temporally fast). Increasing H further up to the energetically highest possible state ($\Theta = 90$, $\Phi = 30$) it decreases (temporally slow process). At and beyond this point because of the threefold degeneracy all
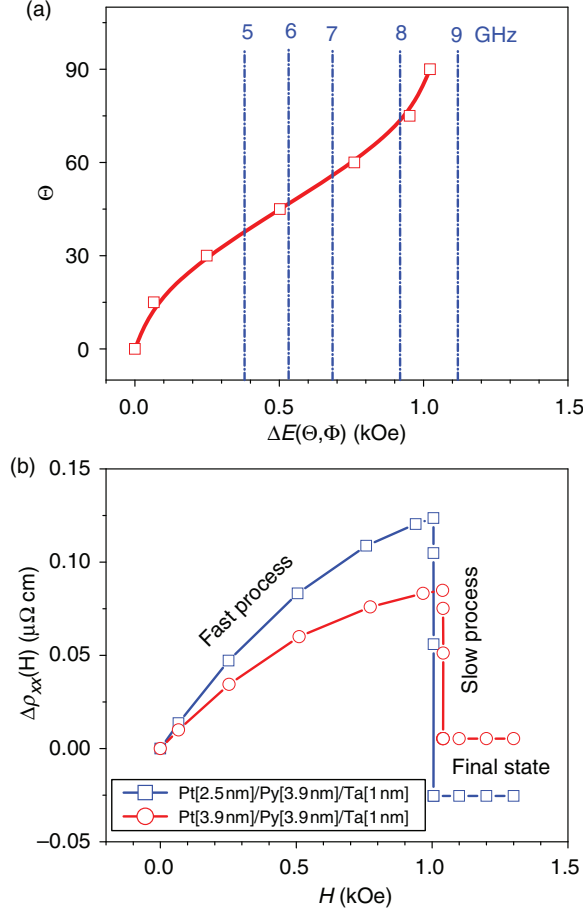
Figure 4. (Color online). (a): Θ versus $\Delta E(\Theta, 0)$ displayed for Pt[3.7 nm]Py[3.9 nm]Ta[1 nm]. The calibration of the resonance frequencies (GHz) in terms of the resonant field H_0 as given in [1] is shown as vertical lines. (b) Difference resistivity as an implicit function $\Delta\rho_{xx}(H)$ of the applied external magnetic field H, see Equation (4), for Pt[x nm]Py[3.9 nm]Ta[1 nm] with x being 2.5 ($\square$) and 3.7 ($\circ$) nm. The labels "fast" and "slow process" refer to the corresponding switching times, the label "final state" indicates that for values of H beyond the energetically highest accessible magnetic state the difference resistivity remains constant.

$\Delta\rho_{xx}(90, 30 + 60n)$, $n = 0, 1, 2$, are equally likely, which in turn implies that for $H \geq \Delta E(90, 30 + 60n)$ an average over these values ought to be considered,

$$\Delta\rho_{xx}(H \geq \Delta E(90, 30)) = \frac{1}{3}\sum_{n=0}^{n=2}\Delta\rho_{xx}(90, 30 + 60n),$$

since there is no energetically higher state (magnetic configuration) accessible.

Comparing now the above theoretical results with the experimental data in [1] two main features have to be stressed, namely (i) as in the experiment Py[4 nm], with or without Ta caps, does not show any oscillations (resonance) in the electric

properties when applying simultaneously a resonant and an external magnetic field, and (ii) the peak observed in the experiment at about 8–9 GHz for Pt[6 nm]Py[4 nm] corresponds to the break in the theoretical data for Pt[3.7 nm]Py[3.9 nm] at about 1 kOe (Figure 4). According to Figure 4a experimental spectra taken at a frequency of less than about 8 GHz refer to the values of $\Delta E(\Theta, 0)$ corresponding to a value of Θ of less than 90. Taking for example in this figure the case of 6 GHz the corresponding value of Θ is about 45. At this frequency the temporally slow process refers to cuts of $\Delta E(\Theta, \Phi)$ and $\Delta\rho_{xx}(\Theta, \Phi)$ with a plane parallel to the xy-plane at $\Theta = 45$, see Figure 2. In this particular case H would first increase monotonously along the path $[\Theta, 0]$, $\Theta < 45$ and then along $[45, \Phi]$, $\Phi \leq 30$.

Theoretically the "peak width" is determined by the maximal value of the "pure" in-plane anisotropy, $\Delta E(90, 30) - \Delta E(90, 0)$, see Figure 2, in the experiment by the FMR line shape. It should be recalled that of course the period of oscillations in cuts of $\Delta E(\Theta, \Phi)$ with a plane parallel to the xy-plane is also governed by the surface orientation of the systems under investigation. For a (100) surface orientation, e.g., the corresponding in-plane rotational symmetry of an fcc-related system is C_4 and therefore for a given value of Θ, see Figure 4, four peaks in $\Delta E(\Theta, \Phi)$, $0 \leq \Phi \leq 180$, are present. Clearly enough, if Θ approaches zero these peaks vanish.

In [1], the resonance is in essence represented by a Lorentzian function with a particular line width centered H_0, the magnetic field corresponding to a given frequency, and the applied external field H_{ext} serving as variable, see Equation (2) in that paper. In the present theoretical approach for $H_{ext} < H_0$ the difference in resistivity with respect to the ground state increases with increasing H_{ext}. At $H_{ext} = H_0$ a "sudden" jump occurs in the difference resistivity such that for $H_{ext} > H_0$ it changes sign. This change of sign is caused by the different properties of in-plane and out-of-plane resistivities.

7. Conclusion

In conclusion it can be said that the interesting experiment performed in [1] can be explained in terms of *ab initio* free energies and *ab initio* resistivities as obtained by a fully relativistic approach, i.e., on an entirely microscopic level. The temporal aspects of the processes involved follow from a multi-scale procedure using (for a given Gilbert damping factor) *ab initio* related parameters in the Landau–Lifshitz–Gilbert equation. The calculated peak positions agree rather well with the experimental data in particular considering that the experimental samples were grown by magnetron sputter deposition. Even the non-existence of a peak for Py[4 nm] found a consistent explanation. Furthermore, it was pointed out that the whole phenomenon has to be regarded as a typical interface effect. It is quite remarkable that due to different time scales the interplay between in-plane and out-of-plane resistivities causes a sizeable physical effect. Clearly, the experimental spectra can also be interpreted [1] in terms of a phenomenological Landau–Lifshitz–Gilbert equation containing additional terms such as a (macroscopic) classical spin–torque term, which of course in this context is not a consequence of "spin–orbit" interactions, but is simply assumed.

References

[1] L. Liu, T. Moriyama, D.C. Ralph and R.A. Burman, Phys. Rev. Lett. 106 (2011) p.036601 and references therein.

[2] J. Zabloudil, R. Hammerling, L. Szunyogh and P. Weinberger, *Electron Scattering in Solid Matter*, Springer, Berlin, Heidelberg, New York, 2004.

[3] P. Weinberger, *Magnetic Anisotropies in Nanostructured Matter*, CRC, Boca Raton, London, New York, 2008.

[4] P. Weinberger, Phys. Rev. B 81 (2010) p.104417.

[5] P. Weinberger, Phys. Rev. B 83 (2011) p.134413.